Desalination and Water Treatment
www.deswater.com

doi: 10.5004/dwt.2017.1835

64 (2017) 118–126
February

Improved water quality and phenol degradation via a combination of electron-beam irradiation (EBI) and activated carbon fiber (ACF)

Joung-Eun Gu[a,b,†], Guntae Son[c,†], Hongshin Lee[b], Jihyun Park[d],
Young-Nam Kwon[b,*] Seunghwan Lee[c,*]

[a] *Hydro Science and Engineering Research Institute, Korea Institute of Civil Engineering and Building Technology (KICT), Andong 36754, Republic of Korea, email: novelje@gmail.com*
[b] *School of Urban & Environmental Engineering, Ulsan National Institute of Science and Technology (UNIST), Ulsan 689-798, Republic of Korea, Tel. +82-54-843-1826; Fax: +82-54-843-1804; emails: kwonyn@unist.ac.kr (Y.-N. Kwon), novelje@gmail.com (J.-E.Gu), ghdtls@unist.ac.kr (H. Lee)*
[c] *School of Civil & Environmental Engineering, Kumoh National Institute of Technology, Gumi 730-701, Republic of Korea, Tel. +82-54-478-7645; Fax: +82-54-478-7859; emails: dlee@kumoh.ac.kr (S. Lee), so20110@hanmai.net (G. Son)*
[d] *Korea Atomic Energy Research Institute, Daejeon 305-353, Republic of Korea, email: jhpark9815@kaeri.re.kr*

Received 19 September 2014; Accepted 25 July 2016

ABSTRACT

Electron-beam irradiation (EBI) was used to remove phenol in aqueous solution. The removal efficiencies of phenol were determined, and their relationships with the initial phenol concentration, absorbed dose, and electron-beam energy were investigated. The EBI was conducted in air with absorbed doses from 40 to 120 kGy under 0.3, 1, and 2 MeV electron beams. *G*-values were introduced to evaluate the removal of phenol quantitatively and were higher at an absorbed dose of 40 kGy than at 80 or 120 kGy. Dose constants (*K*) were found to depend on the absorbed dose and initial phenol concentration and used to calculate the optimum doses required for 90% ($D_{0.9}$) and 50% ($D_{0.5}$) removal of phenol. The reduction of the biochemical oxygen demand (BOD_5), chemical oxygen demand (COD_{Cr}), and total organic carbon (TOC) via EBI indicated organic degradation upon irradiation. The EBI process was combined with activated carbon fiber (ACF) adsorption to improve the COD_{Cr} removal efficiency. The optimum ACF doses were 0.5, 1.0, and 1.33 g L^{-1} with 3, 6, and 6 h contact times for the 20, 50, and 100 mg L^{-1} phenol solutions, respectively. The combination of EBI with ACF improved the COD_{Cr} removal efficiency, even in the more concentrated phenol solution. EBI may be a promising pretreatment process for purifying highly concentrated wastewater.

Keywords: Electron-beam irradiation; Dose; Phenol; Activated carbon fiber

1. Introduction

Many industries use phenol and substituted phenol in their manufacturing processes. Phenol and phenolic compounds have attracted much attention because of their widespread use and high content in the aqueous effluents of industries, such as those from refineries (5–500 mg L^{-1}), coking operations (28–3,900 mg L^{-1}), and coal processing (9–6,800 mg L^{-1}) [1]. Industrial wastewater containing phenolic compounds has high salinity, acidity, and chemical oxygen demand (COD) [2]. The poor biodegradability, high toxicity, and other ecological properties of phenolic compounds present pollution problems, and they are harmful to human health [2].

In order to remove the phenol and phenolic compounds, various traditional methods such as adsorption and biological processes were used. However, these processes are not efficient enough for phenol removal [3]. Wastewater

---

* Corresponding author.

†Contributed equally to this work.

1944-3994/1944-3986

containing phenolic compounds can be treated with AOPs via photocatalysts (TiO_2/UV), photo-Fenton reactions [4–7], UV radiation (UV/O_3, UV/H_2O_2) [8], and ozonation (O_3, O_3/H_2O_2) [9]. Currently, they are regarded as efficient technologies owing to their effective degradation and specific pollutant removal performances, although the treatment costs and energy demands are high [4,10]. Advanced oxidation processes (AOPs) can be an alternative for the effective removal of recalcitrant pollutants from liquid phase. AOPs are based on generation of hydroxyl radicals (OH•) that oxidizes the organic substances quickly and nonselectively with the rate constants' range of 10^{-6}–10^{-9} M^{-1} s^{-1} [11–13]. The OH• radical is among the strongest oxidizing species used in water and wastewater treatment and offers the potential to greatly accelerate the rates of contaminant oxidation. The generation of OH• radicals is commonly accelerated by combining ozone (O_3), heterogeneous photocatalysis, UV radiation, ultrasound, titanium dioxide (TiO_2), hydrogen peroxide (H_2O_2), and/or high electron-beam irradiation (EBI).

Among these AOPs, EBI has been demonstrated to be effective in removing toxic organic compounds from aqueous solution [4,14–16]. EBI is one of the AOPs based on the generation of OH radicals. EBI has attracted a lot of attention as a green technology. EBI generates hydroxyl radicals to strongly oxidize various hazardous organic compounds [17]. EBI has also been suggested as a technology for treating sludge, surface water, industrial wastewater, and groundwater [18], having poor biodegradability, owing to the potential for application in the aquatic environment. However, the most effective use of EBI seems to be to combine it with a conventional treatment under conditions where some synergistic effects occur. Activated carbon fiber (ACF) with a high surface area has been expected to be an excellent adsorbent for the treatment of polluted water or wastewater [19]. Removal of organic matter from wastewater has previously been carried out using activated carbons. Measures of the gross amount of organic matter in wastewater include the five-day biochemical oxygen demand (BOD_5), COD, and total organic carbon (TOC). These values are useful for estimating wastewater characteristics and treatment efficiency.

In this paper, we report the optimum operating conditions for phenol removal using EBI combined with ACF process (EBI-ACF). At various absorbed doses and phenol concentrations, the removal efficiency and *G*-value were quantitatively estimated using low electron-beam energy. The *G*-value of the phenolic compounds represents the decomposition rate and helps to reveal the maximum efficiency of the EBI process. The removal efficiencies after EBI treatment were evaluated through the BOD_5, COD_{Cr}, and TOC of the phenol solutions. Adsorption dose and contact time of the ACF were optimized for different initial phenol concentrations so that ACF adsorption could be combined with EBI. Finally, EBI, ACF, and the combination of the two were compared in terms of their COD_{Cr} removal efficiencies.

2. Experimental

For this study, phenol solutions were prepared on various concentrations. Each sample was treated by EBI, ACF, and EBI combined with ACF process. The description of experimental setup is shown in Fig. 1.

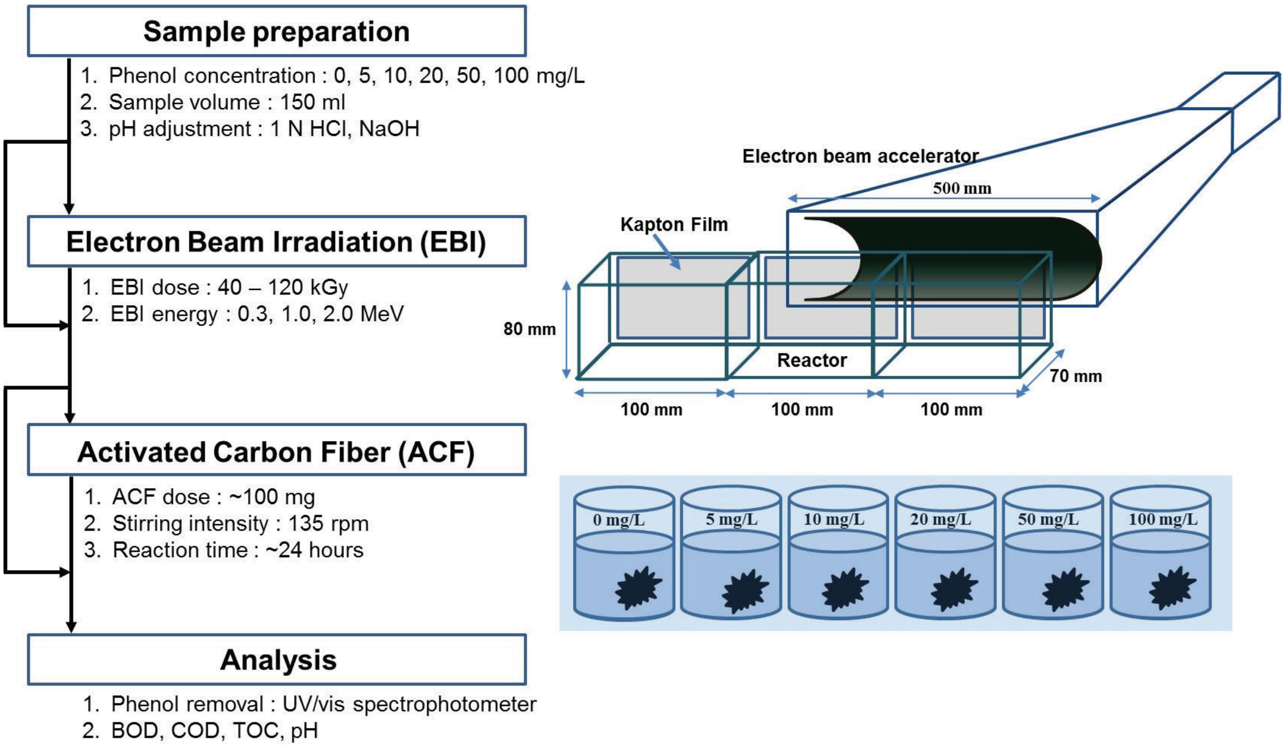

Fig. 1. Flow diagram of EBI, ACF and EBI combined with ACF processes for phenol decomposition.

2.1. Electron-beam irradiation

The electron accelerator (KAERI, Korea) used in this study was the horizontal version with a 100-kW beam power. The distance from the beam source to the sample was 10 cm. The phenol solution was irradiated and stirred with a mixing rate of 275 rpm to compensate due to the low penetration depth [20]. The average dose rate was 0.56 kGy s^{-1}. The observed dose was adjusted to be in the 40–120 kGy range by changing the irradiation time and measured using a Genesys 20 batch dosimeter (Thermo Scientific Co., USA) and dosimetry film (B3 WINdose dosimetry, GEX Co., USA). The irradiations were conducted with energies of 0.3, 1, and 2 MeV at room temperature. The length, width, and height of the reactor used in these experiments were 100, 70, and 80 mm, respectively. The reactors were made of polypropylene with a 70 × 50 mm square window covered by a 0.6-μm Kapton film.

2.2. Materials and methods

Phenol (98%) was purchased from Daejung Co., Ltd, Korea. Phenol solutions were prepared by mixing phenol with distilled water at the prescribed concentrations, in the 5–100 mg L^{-1} range. The studied phenol concentrations were obtained by diluting the standard solution. In the reactors, 150 mL phenol solutions were irradiated by a single irradiation dose.

The ACF with a Brunauer–Emmett–Teller (BET) surface area of 1,000 m^2 g^{-1} was supplied by ACF, Korea. It has a bulk density of 0.2 kg m^{-3} and an iodine number of 1,500 mg g^{-1}. The direct photometric method was used to determine the COD_{Cr}. The BOD_5 was analyzed according to the Standard Methods of Analysis [21]. For the BOD_5 measurements, the samples were incubated at 20 ± 1°C in 300 mL Winkler bottles. The TOC was measured by a TOC analyzer (TOC-5000A, Shimadzu, Japan). The pH was adjusted to the desired value with 1 N HCl or 1 N NaOH solution and measured using a glass electrode method. The concentrations of phenol were quantitatively analyzed with a UV/vis detector (Humas, Korea) in the 0.1–10 mg L^{-1} range at 510 nm. Its photometric repeatability was less than ±0.002 Abs.

2.3. G-value and dose constant

The removal efficiencies are difficult to compare through fixed quantity parity. The removal of organic compounds after irradiation was described by the destruction *G*-value (G_D), defined as the decomposition of the solute in an aqueous solution. In order to quantitatively describe the removal of phenol, the *G*-value was calculated. The *G*-value for solute removal at a given dose G_D is determined experimentally using Eq. (1) [22]:

$$G_D = \frac{[\Delta R]\mathrm{N}_A}{D \times 6.24 \times 10^{19}} \tag{1}$$

where ΔR represents the change in the phenol concentration (mol J^{-1}) at a given dose while D and 6.24×10^{19} are the dose (kGy) and the conversion factor from kGy to 100 eV L^{-1}, respectively. N_A represents Avogadro's number. For the G_D calculation, the minimum dose required to achieve 90% and 50% removal of each pollutant was considered.

Calculation of the dose constant was performed by taking the slope of the line obtained from the plot of the natural logarithm of the phenol concentration vs. the dose. The dose constant (*K*) was used to calculate the amount of radiation required to achieve the desired changes in the phenol concentration. *K* was determined using Eqs. (2) and (3).

$$C = C_0 e^{-KD} \tag{2}$$

$$\mathrm{In}\left(\frac{\mathrm{C}_0}{\mathrm{C}}\right) = \mathrm{KD} \tag{3}$$

where C_0 and C represent the phenol concentrations before and after irradiation, respectively. D represents the absorbed dose required to achieve the desired concentration change, while K is the dose constant obtained from the plot of the concentration vs. dose. The K value can be considered as an ideal figure for the comparison of irradiation applications [23].

2.4. Adsorption of phenol onto ACF

Batch adsorption experiments were conducted for the adsorption of phenol onto ACF. The adsorption test to determine for the optimum time for equilibrium adsorption was conducted by shaking flasks containing 150 mL of phenol solution and 100 mg of adsorbent in an incubated shaker at 135 rpm. Similarly, batch isotherm experiments were conducted by shaking flasks containing 100 mg of ACF and different concentrations of phenol for 24 h in an incubated shaker at 25°C. The phenol concentration was measured before the adsorption, and the equilibrium concentration was measured after the adsorption. The quantity of adsorbed phenol at equilibrium was calculated using Eq. (4):

$$q = \frac{(C_0 - C_e) \times V}{W} \tag{4}$$

where q is the quantity of solute adsorbed; C_0 is the initial phenol concentration (mg L^{-1}); C_e is the equilibrium phenol concentration (mg L^{-1}); V is the volume of the solution (L); and W is the mass of the adsorbent (mg).

The adsorption capacity at equilibrium (mg g^{-1}), qe, was determined from the plot of adsorbed phenol against ACF dose and used to determine the optimum contact time in EBI combined with ACF.

3. Results and discussion

3.1. Effect of irradiation dose and EBI energy

According to previous studies [17,24,25], three main reactive species are formed as a result of electron irradiation in aqueous solution: aqueous electrons (e_{aq}^-), hydrogen atoms (H•), and hydroxyl radicals (OH•). The radical species formed via radiolysis can degrade organic pollutants, provided that the irradiation dose is sufficient.

The characteristics of decomposition of phenol by EBI with various doses and energies are shown in Fig. 2. It was observed that the phenol decomposition increased with an increase in the absorbed dose and a decrease in the initial concentration at 0.3 MeV (Fig. 2(a)). The main factors affecting phenol removal are the initial concentration and the irradiation dose. The value of C/C_0 in the figures indicates the ratio of the phenol concentrations after and before irradiation. The removal efficiencies of phenol decrease despite the continuous increase in the irradiation dose. The concentration of phenol decreased sharply with increasing irradiation dose until 80 kGy (except 100 mg L^{-1} phenol), at which point the phenol concentration began to decrease slowly. In general, the concentration of phenol did not decrease linearly despite the increase in absorbed dose. This trend had been reported in Kim's (2002) study for toluene [26]. The nonlinearity of these curves may be attributed to collision disturbances with phenol molecules or back reactions between abundant radicals [17,27]. In particular, the hydroxyl radical would be expected to be a main reactive species since previous research papers have estimated that most of the radicals in the destruction of pollutants by electron irradiation are hydroxyl radicals [4,17,28].

Radical products such as OH•, e^-_{aq}, and H• produced via the EBI react with and degrade phenol [17]. Phenol attacked by these radicals may lose a hydrogen ion, and hence, the pH of the solution may decrease. The pH of the aqueous solution after irradiation decreased from 6.8 to 5.0, 4.3, and 4.1 at 40, 80, and 120 kGy, respectively, at an irradiation energy of 0.3 MeV. It has been reported that the decrease in pH resulting from the reaction between phenol and these radicals is due to the decomposition products of phenol being mainly catechol and hydroquinone [4,29,30]. This also led to decreases in pH from 4.0 to 3.7, 3.7, and 3.7; and from 10.0 to 7.9, 8.5, and 8.5 for the 20, 50, and 100 mg L^{-1} phenol solutions, respectively, at 80 kGy and 0.3 MeV.

The removal efficiencies of phenol under various electron beam (EB) energies are shown in Fig. 2(a). At 40 kGy, phenol degradation increased with an increase in the EB energy. As shown in Fig. 2(b), the phenol removal curve at an absorbed dose of 40 kGy showed the sharpest drop. Therefore, a 40-kGy absorbed dose was chosen to assess the effect of the EB energy. At an EB energy of 1 MeV, degradation of 50 mg L^{-1} phenol was 3.8 times greater than that at 0.3 MeV. A decomposition rate of over 90% for phenol was observed when using EB energies of 1 and 2 MeV, and the degradations of phenol at these energies were similar. An EB energy of 1 MeV was sufficient to obtain the desired phenol decomposition rate. In addition, an EB energy of 0.3 MeV was enough to remove low concentrations of phenols.

3.2. Phenol removal efficiency (G_D) and dose constant (K)

The removal of phenol via EBI can be quantified by the G-value (G_D). Table 1 shows the degradation efficiency (G_D) and dose constants (K) of phenol at various initial concentrations. K was calculated from the slope of the regression line of the residual curves, obtained by plotting the log residual (C/C_0) (Fig. 3). The doses required to achieve 90% ($D_{0.9}$) and 50% ($D_{0.5}$) removal of phenol were calculated using K (Eqs. (5) and (6)); the results are shown in Table 1.

$$D_{0.5} = \text{In}\,2 / K \tag{5}$$

$$D_{0.9} = \text{In}\,10 / K \tag{6}$$

The G-value was calculated at various initial phenol concentrations. In radiation chemistry, G-values are defined as the number of molecules lost or formed for every 100 eV absorbed by the system. Therefore, another quantitative descriptor of the removal efficiency is the radiation chemical yield G_D, which is the G-value for the loss of phenol at a given dose (D) [17]. As shown in Fig. 4, the G-value increased with

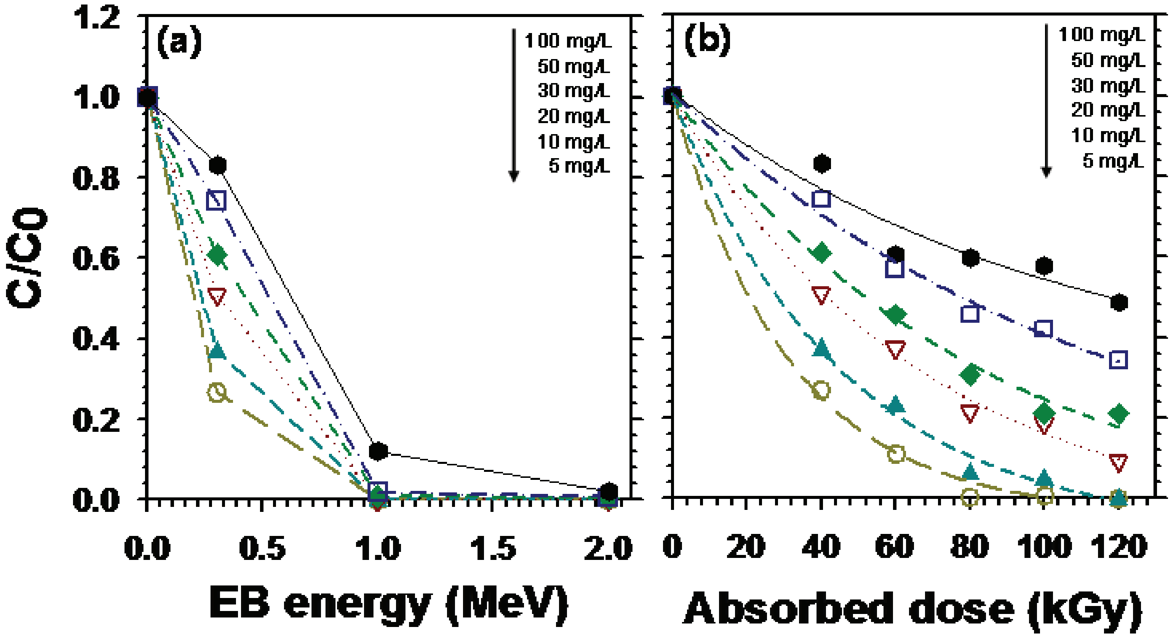

Fig. 2. Degradation of phenol as a function of (a) the EB energy (absorbed dose = 40 kGy) and (b) the absorbed dose (EB energy = 0.3 MeV).

Table 1
Summary of phenol removal at different initial phenol concentrations and dose constants

Phenol concentration (mg L^{-1})	Irradiation energy = 0.3 MeV			
	^{a}K	$^{b}R^2$	$^{c}D_{0.5}$	$^{d}D_{0.9}$
5	0.053	0.86	13.2	43.7
10	0.030	0.96	22.8	75.7
20	0.019	0.98	37.5	124.5
30	0.014	0.97	49.5	164.5
50	0.009	0.99	77.0	255.8
100	0.006	0.93	113.6	377.5

^{a}K = dose constant.
$^{b}R^2$ = coefficient of determination.
$^{c}D_{0.5}$ = the absorbed dose required to remove the 50% of the initial phenol concentration.
$^{d}D_{0.9}$ = the absorbed dose required to remove the 90% of the initial phenol concentration.

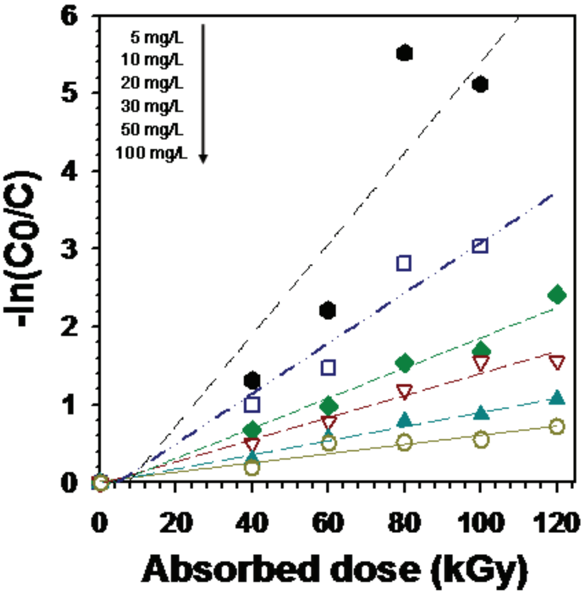

Fig. 3. Pseudo-first-order decay of phenol removal in response to various EBI doses (EB energy = 0.3 MeV).

a decrease in dosage and an increase in energy. As previously observed with cefaclor [31], chloroform, and methyl tert-butyl ether (MTBE) [32], the reactive radicals produced from water through EBI have a higher chance of reacting with phenol in a more concentrated phenol solution, as indicated by the *G*-value. It seems that a high initial concentration of phenol leads to high decomposition efficiency, as shown in Fig. 3.

The gray, as a unit of dose, indicates the energy of the absorbed radiation per kilogram of matter. The removal efficiency of phenol, defined by the *G*-value, is shown in Fig. 4. The *G*-value decreased with increasing absorbed dose and decreasing phenol concentration under the same EB energy. At an EB energy of 0.3 MeV, the *G*-value initially increased proportionally with the concentration of phenol and then increased gradually. In particular, the *G*-value at a low irradiation dose, 40 kGy, showed a slight increase with increasing phenol concentration. The *G*-value is lowers with the increasing absorbed dose according to the increasing recombination of the active species, and eventually the removal efficiency drops [17,33].

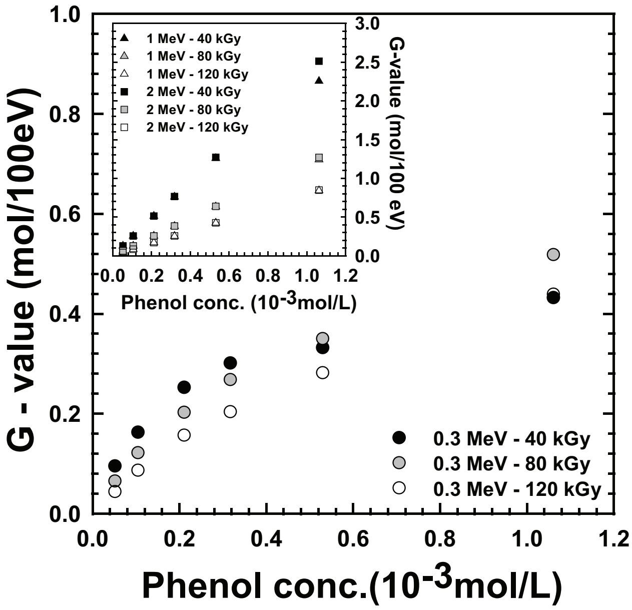

Fig. 4. *G*-values (G_D) at different EBI energies (MeV) and doses (kGy).

The phenol removal efficiency increases with increasing EB energy. However, an EB energy of 2 MeV produced only a slightly higher *G*-value than that at 1 MeV, which produced a *G*-value that was distinctly higher than that at 0.3 MeV. This means that the removal efficiency is not proportional to the EB energy. The *G*-value graphs at low concentrations of phenol show similar gradients at 40 and 80 kGy doses and EB energies of 0.3, 1, and 2 MeV. Therefore, the extent of degradation was found to increase nonlinearly with the EB energy.

The minimum doses required to obtain 90% and 50% removal were denoted as $D_{0.9}$ and $D_{0.5}$, respectively. The *K* values obtained in Fig. 3 were used to calculate $D_{0.9}$ and $D_{0.5}$ using Eqs. (5) and (6), and the results are shown in Table 1.

These data were collected for six different concentrations. For 20 mg L^{-1} phenol, 50% and 90% degradation corresponded to absorbed doses of 38 and 125 kGy, respectively. These results may be taken as the doses required to treat wastewater with the target concentration using a 0.3-MeV electron beam. In this study, an EB energy of 0.3 MeV was used to measure the variation in the BOD, COD$_{Cr}$, and TOC during phenol removal.

3.3. Water quality improvement via EBI

A series of experiments was conducted to study the effects of EBI on the degradation of organics, that is, BOD$_5$, COD$_{Cr}$, and TOC, via the radiolytic decomposition of phenol. These parameters are used to quantify organic material in wastewater.

The BOD$_5$ was monitored for different phenol concentrations, as shown in Fig. 5(a). After EBI, the BOD$_5$ values

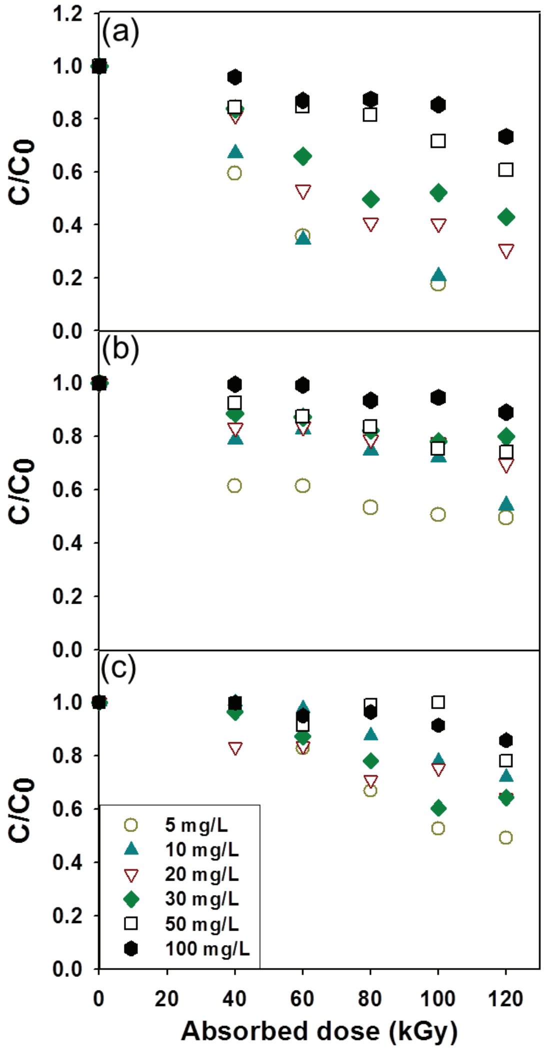

Fig. 5. Variation of (a) BOD_5, (b) COD_{Cr}, and (c) TOC at various initial phenol concentrations (EB irradiation energy = 0.3 MeV).

for initial concentrations of 20, 30, 50, and 100 mg L^{-1} were reduced by 69%, 57%, 40%, and 27%, respectively. The removal efficiency decreased with an increase in the initial concentration. These results are due to conversion of degraded phenol into organic acids, which are hardly biodegradable. The main reaction leading to phenol degradation will be the one involving the hydroxyl radical as mentioned above [4]. The reported stable products of the reaction are mainly catechol and hydroquinone [4,34,35]. These organic acids are also responsible for the lower pH, as mentioned in section 3.1.

The variations in COD_{Cr} and TOC under various conditions are shown in Figs. 5(b) and(c). The reductions in COD_{Cr} of 10 mg L^{-1} phenol were 21% and 46% at 40 and 120 kGy doses, respectively. Reductions of 22% and 14% in the TOC were observed in the 50 and 100 mg L^{-1} phenol solutions, respectively, after irradiation at a dose of 120 kGy. It is clear that the removal of organics from the phenol solutions increased with an increase in the absorbed dose. BOD_5 showed a larger decrease than COD_{Cr} after irradiation. This is considered to be because chemically degradable materials were involved more than biologically degradable materials were in the untreated phenol solution and were decomposed by the EB-formed radicals. The reduction in TOC was lower than those in BOD_5 and COD_{Cr}. Phenol is known to decompose or be converted into intermediate species by radicals. Radicals produced through EBI decompose several types of intermediates produced in the course of phenol decomposition and mineralize into CO_2 and H_2O.

The BOD_5/COD_{Cr} ratio is commonly used as a biodegradability measure [36–38]. At initial phenol concentration of 50 and 100 mg L^{-1}, it was observed that the reduction in the BOD_5 with a low absorbed dose was lower than that observed in COD_{Cr} with a higher dose at an initial phenol concentration of 100 mg L^{-1}. This result indicates high biodegradability after high-dose EBI. For phenol concentrations lower than 50 mg L^{-1}, the reduction in BOD_5 was greater than that in COD_{Cr}. Low concentration phenol solutions show high biodegradability after irradiation because the radicals produced through EBI are sufficient to remove the decomposed and biodegradable phenol intermediates.

However, the more concentrated phenol solution showed low biodegradability and a high COD_{Cr} value as an estimate of the extent of chemical oxidation at low-dose EBI. This indicates that the phenol intermediates produced after EBI are more difficult to remove via biological treatment in the case of high concentrations of phenol, whereas the EB process can lead to high biodegradability at low concentrations of phenol with a low EB dose.

3.4. Adsorption of phenol by ACF

The above results showed that there was an improvement in water quality along with an actual reduction in organics after EBI treatment. Degradation of the phenol solution through EBI even produces intermediates. In this study, ACF adsorption was combined with EBI. The optimum dose of ACF was determined for 20, 50, and 100 mg L^{-1} phenol solutions. The adsorption experiments with ACF were carried out in an incubator with a mixing speed of 135 rpm and a 150 mL sample. For phenol concentrations of 20, 50, and 100 mg L^{-1}, the optimum adsorption uptakes, *qe*, were 0.5, 1.0, and 1.33 g L^{-1}, respectively (Fig. 6(a)). After determining the optimum dose of ACF, another series of experiments was conducted to determine the optimum contact time. In this experiment, samples were collected at various times ranging from 5 to 1,440 min. Fig. 6(b) shows the effects of the agitation time and initial phenol concentration on the adsorption by activated carbon at 25°C. The adsorption of phenol initially increased with increasing time and then leveled off.

At equilibrium, the amount of phenol desorbed from the activated carbon was in a state of dynamic equilibrium with the amount of adsorbed phenol. The amount of phenol adsorbed at the equilibrium time reflects the maximum adsorption uptake of the activated carbon. Based on these experiments, the removal efficiencies of organic compounds were calculated for the ACF adsorption process. Phenol adsorption combined with EBI was conducted with ACF doses of 0.5, 1.0, and 1.33 g L^{-1} at 25°C and at the optimum contact times of 3, 6, and 6 h for phenol concentrations of 20, 50, and 100 mg L^{-1}, respectively.

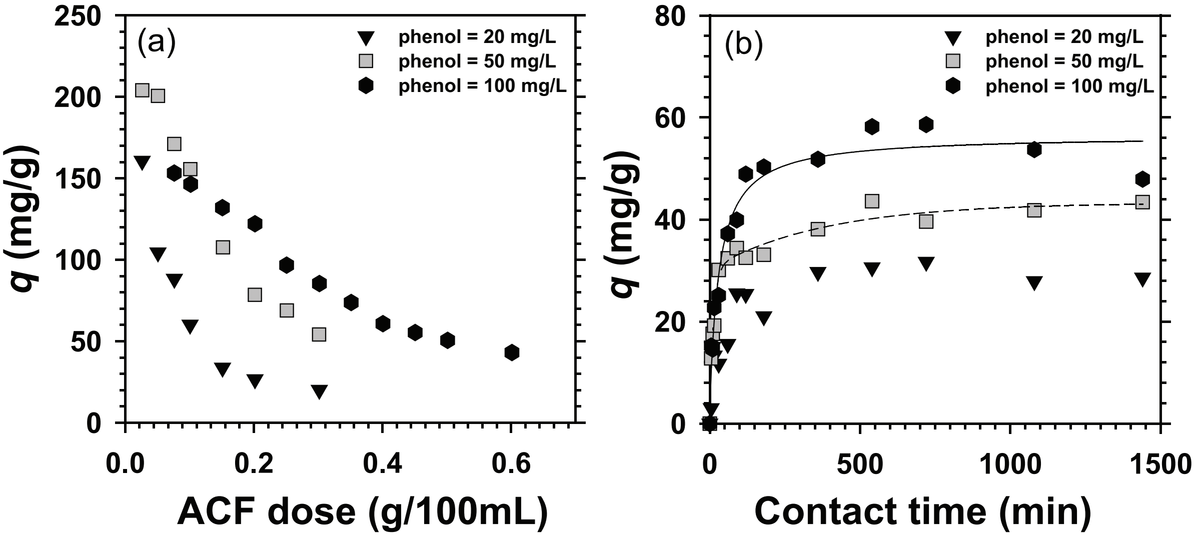

Fig. 6. Phenol adsorption as a function of (a) the ACF doses for 24 h and (b) the contact time with ACF dose of 0.5, 1.0, and 1.33 g L^{-1} for phenol concentrations of 20, 50, and 100 mg L^{-1}, respectively (agitation speed = 135 rpm, temperature = 25°C).

3.5. Removal of organic compounds via EBI combined with ACF

The adsorption behavior of porous carbon materials such as activated carbon is of great interest because of their relevance in various areas such as pollution control, heterogeneous catalysis, and gas and energy storage. Different carbon materials have also been widely used in treatment processes for drinking water and wastewater. ACF is a porous carbon with a fibrous shape and a well-defined porous structure, and is a very promising material because of its high adsorption capacity and rate. It is highly microporous with little or no mesoporosity, and has a large specific surface area. Another important advantage of ACF is that it can be produced in different physical forms, such as fiber tows, fabrics, and felts, enabling easy handling for specific purposes [39].

The decrease in the COD_{Cr} in response to the combined EBI-ACF treatment for phenol concentrations of 20, 50, and 100 mg L^{-1} is illustrated in Fig. 7. As mentioned above, the COD_{Cr} of the more concentrated phenol solution showed a slight reduction under a 0.3 MeV electron beam. In this study, 1 and 2 MeV electron beams were applied to measure the notable degradation of COD_{Cr} through EBI, ACF, and the EBI-ACF process. The ACF adsorption process was conducted at ACF doses of 0.5, 1, and 1.33 g L^{-1} and adsorption times of 3, 6, and 6 h for initial phenol concentrations of 20, 50, and 100 mg L^{-1}, respectively.

The decreases in the COD_{Cr} of the phenol solutions under 1 and 2 MeV EBI showed a similar tendency to that under 0.3 MeV EBI. The COD_{Cr} of the 20 mg L^{-1} phenol solution decreased more than those of the 50 and 100 mg L^{-1} phenol solutions. A 61.7% COD_{Cr} degradation was achieved for the 20 mg L^{-1} phenol solution at a 120 kGy dose under 1 and 2 MeV EBI. The 50 and 100 mg L^{-1} phenol solutions at a 120 kGy dose showed COD_{Cr} degradation of 26.6% and 15.2% at 1 MeV and 49.8% and 22.4% at 2 MeV, respectively. ACF adsorption showed high COD_{Cr} removal owing to the optimized adsorption dose and contact time for the 50 and 100 mg L^{-1} phenol solutions. The improved COD_{Cr} removal efficiency can be ascribed to the adsorption of by-products from phenol dissociation. The combined EBI-ACF process at an EB energy of 2 MeV showed improved removal efficiencies for the 100 mg L^{-1} phenol solution of 97.2%, 98.5% and 99.8% at 40, 80, and 120 kGy doses, respectively. This result indicates that the EBI-ACF process could improve COD_{Cr} removal efficiency even in the more concentrated phenol solution.

Recently, there has been much research on radiolytic degradation for wastewater treatment using ozonation, UV light, gamma-ray irradiation and electron beams. Kim et al. (2012) studied the removal of antibiotics using an electron beam, ozone and UV light, and reported that the electron beam was more efficient than ozonation and UV light based on the electrical energy [40]. Emani-Meibodi et al. (2016) reported the effect of ozonation together with an electron beam and revealed that EB irradiation may be the most suitable in industrial scale operations [41]. The combined EBI-ACF process led to improved water quality parameters such as above studies and can produce treated water suitable for industrial reuse. However, the treatment conditions and efficiencies need to be optimized to increase for the cost-effectiveness of the process.

4. Conclusion

A combined EBI-ACF process was used to treat phenol and phenol by-products. It was shown that EBI can effectively remove phenol from aqueous solutions. The extent of phenol removal was determined by the initial phenol concentration, absorbed dose, and EB energy. The radiation chemical yield, G_D, was estimated to quantitatively describe the phenol removal. The optimum doses required to achieve 90% ($D_{0.9}$) and 50% ($D_{0.5}$) removal of phenol were calculated using the K constant. With 1 and 2 MeV electron beams, the G-value was proportional to the phenol concentration. However, at an EB energy of 0.3 MeV, the G-value was not proportional

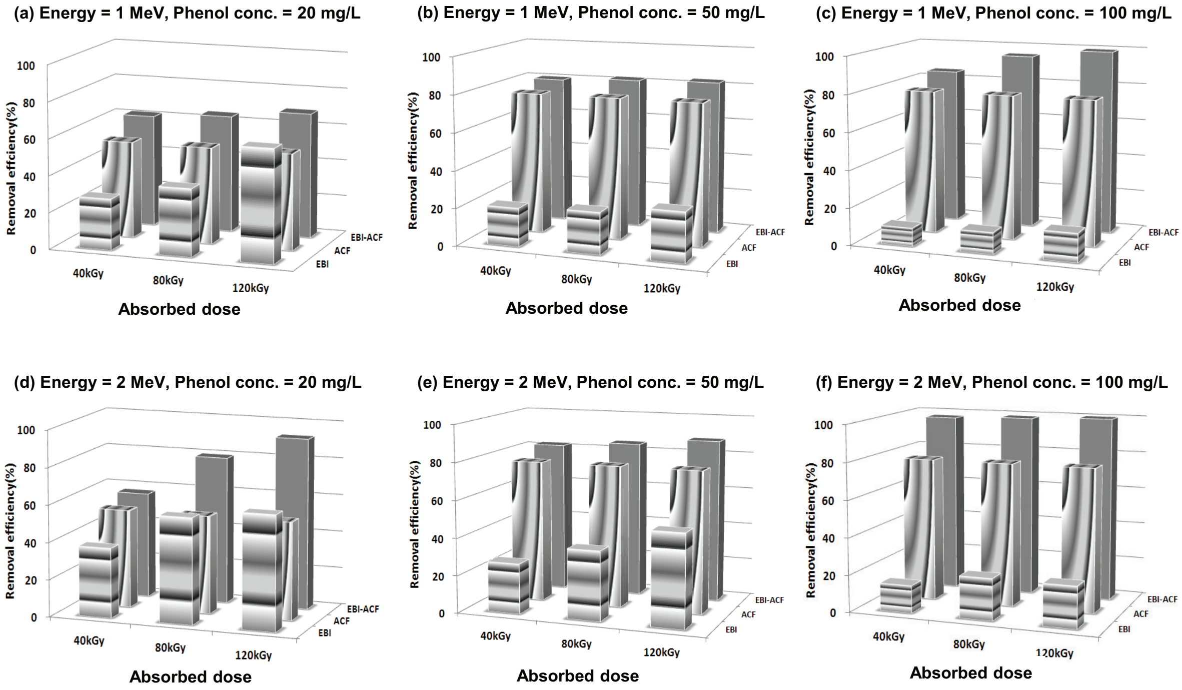
(a) Energy = 1 MeV, Phenol conc. = 20 mg/L
(b) Energy = 1 MeV, Phenol conc. = 50 mg/L
(c) Energy = 1 MeV, Phenol conc. = 100 mg/L
(d) Energy = 2 MeV, Phenol conc. = 20 mg/L
(e) Energy = 2 MeV, Phenol conc. = 50 mg/L
(f) Energy = 2 MeV, Phenol conc. = 100 mg/L

Fig. 7. Comparison of COD_{Cr} removal efficiency using EBI, ACF, and EBI-ACF processes of (a) 20 mg L^{-1}, (b) 50 mg L^{-1}, and (c) 100 mg L^{-1} phenol solutions under 1 MeV EB energy and (d) 20 mg L^{-1}, (e) 50 mg L^{-1}, and (f) 100 mg L^{-1} phenol solutions under 2 MeV EB energy (ACF dose = 0.5, 1.0, and 1.33 g L^{-1}, contact time = 3, 6, and 6 h for 20, 50, and 100 mg L^{-1} phenol solutions, respectively).

to the phenol concentration, because a low EB energy is not sufficient to remove phenol at a high concentration.

The minimum doses required to obtain 90% and 50% removal with a 0.3 MeV electron beam were 38 and 125 kGy, respectively. The BOD_5, COD_{Cr}, and TOC were estimated to study the effects of EBI on the degradation of the organics through the radiolytic decomposition of phenol.

Low concentration phenol solutions showed high biodegradability when comparing the removal efficiencies in terms of the BOD_5 and COD_{Cr}. However, a high concentration of phenol resulted in low biodegradability with a low COD_{Cr} because of the presence of phenol decomposition intermediates. The EBI process was combined with the ACF process to improve the removal efficiency in terms of the COD_{Cr}. Optimum ACF doses of 0.5, 1.0, and 1.33 g L^{-1} and contact times of 3, 6, and 6 h were used for initial phenol concentrations of 20, 50, and 100 mg L^{-1}, respectively. The EBI-ACF process improved COD_{Cr} removal efficiency even in the more concentrated phenol solution. EBI may be a promising pretreatment process for purifying highly concentrated wastewater.

Acknowledgment

This work was supported by the Nuclear R&D Program of the Ministry of Science and Technology, Republic of Korea.

References

[1] G. Busca, S. Berardinelli, C. Resini, L. Arrighi, Technologies for the removal of phenol from fluid streams: a short review of recent developments, J. Hazard. Mater., 160 (2008) 265–288.

[2] L.J. Kennedy, J.J. Vijaya, K. Kayalvizhi, G. Sekaran, Adsorption of phenol from aqueous solutions using mesoporous carbon prepared by two-stage process, Chem. Eng. J., 132 (2007) 279–287.

[3] B. Marrot, A. Barrios-Martinez, P. Moulin, N. Roche, Biodegradation of high phenol concentration by activated sludge in an immersed membrane bioreactor, Biochem. Eng. J., 30 (2006) 174–183.

[4] N. Chitose, S. Ueta, S. Seino, T.A. Yamamoto, Radiolysis of aqueous phenol solutions with nanoparticles. 1. Phenol degradation and TOC removal in solutions containing TiO_2 induced by UV, γ-ray and electron beams, Chemosphere, 50 (2003) 1007–1013.

[5] P. Jin, R. Chang, D. Liu, K. Zhao, L. Zhang, Y. Ouyang, Phenol degradation in an electrochemical system with TiO_2/activated carbon fiber as electrode, J. Environ. Chem. Eng., 2 (2014) 1040–1047.

[6] A. Barrera, F. Tzompantzi, J.M. Padilla, J.E. Casillas, G. Jácome-Acatitla, M.E. Cano, R. Gómez, Reusable $PdO/Al_2O_3–Nd_2O_3$ photocatalysts in the UV photodegradation of phenol, Appl. Catal., B, 144 (2014) 362–368.

[7] R.C. Martins, A.F. Rossi, R.M. Quinta-Ferreira, Fenton's oxidation process for phenolic wastewater remediation and biodegradability enhancement, J. Hazard. Mater., 180 (2010) 716–721.

[8] C.K. Scheck, F.H. Frimmel, Degradation of phenol and salicylic acid by ultraviolet radiation/hydrogen peroxide/oxygen, Water Res., 29 (1995) 2346–2352.

[9] M.S. Lucas, J.A. Peres, G.L. Puma, Treatment of winery wastewater by ozone-based advance oxidation prosesses (O_3, O_3/UV and $O_3/UV/H_2O_2$) in a pilot-scale bubble column reactor and process economics, Sep. Purif. Technol., 72 (2010) 235–241.

[10] N.N. Mahamuni, Y.G. Adewuyi, Advanced oxidation processes (AOPs) involving ultrasound for waste water treatment: a review with emphasis on cost estimation, Ultrason. Sonochem., 17 (2010) 990–1003.

[11] R. Andreozzi, V. Caprio, A. Insola, R. Marotta, Advanced oxidation processes (AOP) for water purification and recovery, Catal. Today, 53 (1999) 51–59.

[12] S. Das, P.V. Kamat, S. Padmaja, V. Au, S.A. Madison, Free radical induced oxidation of the azo dye Acid Yellow 9, J. Chem. Soc. Perkin Trans., 2 (1999) 1219–1224.

[13] Y. Yang, D.T. Wyatt II, M. Bahorsky, Decolorization of dyes using UV/H_2O_2 photochemical oxidation, Text. Chem. Color, 30 (1998) 27–35.

[14] N.J. Drenzek, M.C. Nyman, N.L. Clesceri, R.C. Block, J.A. Stenken, Liquid chromatographic aqueous product characterization of high-energy electron beam irradiated 2-chlorobiphenyl solutions, Chemosphere, 54 (2004) 387–395.

[15] T.-M. Ting, N.A. Jamaludin, Decolorization and decomposition of organic pollutants for reactive and disperse dyes using electron beam technology: effect of the concentrations of pollutants and irradiation dose, Chemosphere, 73 (2008) 76–80.

[16] B.G. Kwon, E. Kim, J.H. Lee, Pentachlorophenol decomposition by electron beam process enhanced in the presence of Fe(III)-EDTA, Chemosphere, 74 (2009) 1335–1339.

[17] K. Lin, W.J. Cooper, M.G. Nickelsen, C.N. Kurucz, T.D. Waite, Decomposition of aqueous solutions of phenol using high energy electron beam irradiation—a large scale study, Appl. Radiat. Isot., 46 (1995) 1307–1316.

[18] S.I. Borrely, A.C. Cruz, N.L. Del Mastro, M.H.O. Sampa, E.S. Somessari, Radiation processing of sewage and sludge. A review, Prog. Nucl. Energ., 33 (1998) 3–21.

[19] A. Czyżewski, J. Karolczyk, A. Usarek, J. Przepiórski, Removal of two ionic dyes from water by MgO-loaded porous carbons prepared through one-step process from poly (ethylene terephthalate)/magnesium carbonate mixtures, Bull. Mater. Sci., 35 (2012) 211–219.

[20] C.N. Kurucz, T.D. Waite, W.J. Cooper, The Miami electron beam research facility: a large scale wastewater treatment application, Radiat. Phys. Chem., 45 (1995) 299–308.

[21] APHA, AWWA, Standard Methods for the Examination of Water and Wastewater, 21th ed., 2005.

[22] C.N. Kurucz, T.D. Waite, W.J. Cooper, M.J. Nickelsen, High energy electron beam irradiation of water, wastewater and sludge, Adv. Nucl. Sci. Tech., 22 (1991) 1–43.

[23] B.J. Mincher, R.R. Brey, R.G. Rodriguez, S. Pristupa, A. Ruhter, Increasing PCB radiolysis rates in transformer oil, Radiat. Phys. Chem., 65 (2002) 461–465.

[24] M.G. Nickelsen, W.J. Cooper, C.N. Kurucz, T.D. Waite, Removal of benzene and selected alkyl-substituted benzenes from aqueous solution utilizing continuous high-energy electron irradiation, Environ. Sci. Technol., 26 (1992) 144–152.

[25] J.W.T. Spinks, R.J. Woods, An Introduction to Radiation Chemistry, 3rd ed., John-Wiley and Sons, Inc., New York, Toronto, 1990.

[26] J.-C. Kim, Factors affecting aromatic VOC removal by electron beam treatment, Radiat. Phys. Chem., 65 (2002) 429–435.

[27] H.-R. Paur, H. Mätzing, K. Woletz, Removal of volatile organic compounds from industrial offgas by irradiation induced aerosol formation, J. Aerosol Sci., 22 (1991) S509–S512.

[28] M.G. Nickelsen, W.J. Cooper, K. Lin, C.N. Kurucz, T.D. Waite, High energy electron beam generation of oxidants for the treatment of benzene and toluene in the presence of radical scavengers, Water Res., 28 (1994) 1227–1237.

[29] G. Stein, J. Weiss, Some free-radical reactions of phenol. The action of the hydrogen peroxide–ferrous salt reagent and of X-rays on aqueous solutions of phenol, J. Chem. Soc., 723 (1951) 3265–3274.

[30] P. Neta, R.W. Fessenden, Hydroxyl radical reactions with phenols and anilines as studied by electron spin resonance, J. Phys. Chem., 78 (1974) 523–529.

[31] S. Yu, B. Lee, M. Lee, I.-H. Cho, S.-W. Chang, Decomposition and mineralization of cefaclor by ionizing radiation: kinetics and effects of the radical scavengers, Chemosphere, 71 (2008) 2106–2112.

[32] A.A. Basfar, H.M. Khan, A.A. Al-Shahrani, W.J. Cooper, Radiation induced decomposition of methyl tert-butyl ether in water in presence of chloroform: kinetic modelling, Water Res., 39 (2005) 2085–2095.

[33] T. Goulet, J.P. Jay-Gerin, On the reactions of hydrated electrons with OH• and H_3O^+•. Analysis of photoionization experiments, J. Chem. Phys., 96 (1992) 5076–5087.

[34] S. Hashimoto, T. Miyata, W. Kawakami, Radiation-induced decomposition of phenol in flow system, Radiat. Phys. Chem., 16 (1980) 59–65.

[35] Z. Guo, R. Ma, G. Li, Degradation of phenol by nanomaterial TiO_2 in wastewater, Chem. Eng. J., 119 (2006) 55–59.

[36] E. Gilbert, Biodegradability of ozonation products as a function of COD and DOC elimination by the example of humic acids, Water Res., 22 (1988) 123–126.

[37] A. Marco, S. Esplugas, G. Saum, How and why combine chemical and biological processes for wastewater treatment, Water Sci. Technol., 35 (1997) 321–327.

[38] E. Chamarro, A. Marco, S. Esplugas, Use of Fenton reagent to improve organic chemical biodegradability, Water Res., 35 (2001) 1047–1051.

[39] J. Figueiredo, N. Mahata, M. Pereira, M. Sánchez Montero, J. Montero, F. Salvador, Adsorption of phenol on supercritically activated carbon fibers: effect of texture and surface chemistry, J. Colloid Interface Sci., 357 (2011) 210–214.

[40] T.-H. Kim, S.D. Kim, H.Y. Kim, S.J. Lim, M. Lee, S. Yu, Degradation and toxicity assessment of sulfamethoxazole and chlortetracycline using electron beam, ozone and UV, J. Hazard. Mater., 227–228 (2012) 237–242.

[41] M. Emami-Meibodi, M.R. Parsaeian, R. Amraei, M. Banaei, F. Anvari, S.M.R. Tahami, B. Vakhshoor, A. Mehdizadeh, N. Fallah Negad, S.P. Shirmardi, S.J. Mostafavi, S.M.J. Mousavi, An experimental investigation of wastewater treatment using electron beam irradiation, Radiat. Phys. Chem., 125 (2016) 82–87.